

15

20

25

30



Spatiotemporal dynamics of riparian vegetation NDVI as indicators of bio-hydromorphological interactions

Yuexia Zhou¹, Yuji Toda¹, Runye Zhu²

¹Department of civil and environmental engineering, Nagoya University, Nagoya, Japan ²Zhejiang Institute of Hydraulics and Estuary, Hangzhou, China.

Correspondence to: Yuexia Zhou (zhou@civil.nagoya-u.ac.jp)

Abstract: The Normalized Difference Vegetation Index (NDVI) can be effectively used for monitoring the spatial and temporal dynamics of riparian vegetation. However, quantitative and efficient evaluations of the relationship between NDVI and bio-hydromorphological processes remain limited, particularly in the context of riverine floodplain management, where dense in-channel vegetation can obstruct flow and reduce conveyance capacity. Using 200 cloud-free Sentinel-2 images (2015–2024) for a 20-km reach of the Chikuma River (Japan), we evaluated the utility of NDVI (extracted from Sentinel-2 images) and the greenness index (defined as NDVI > 0.2) as quantitative indicators of bio-hydromorphological interactions, focusing on: (1) the relationship between NDVI dynamics, flood magnitude, and lateral channel morphology of relative elevation, and (2) the seasonal dynamics of riparian vegetation within frequently disturbed channels. Results indicated that NDVI fluctuations strongly corresponded to flood disturbances at lower elevations, while vegetation at higher elevations remained relatively stable. Along cross-channel transects, the maximum greenness ratio was well represented by a logistic model, with parameters varying according to flood magnitude from the previous year. Annual vegetation greenness additionally exhibited clear seasonal cycles, showing a late-summer greenness peak (August–September). The spatial and seasonal characteristics of NDVI displayed its potential as an indicator for operationalizing the "where" (priority bands by relative elevation) and "when" (phenological window) of vegetation control, and offered a transferable, remotely sensed basis for flood-risk mitigation and ecohydraulic planning.

1 Introduction

Riparian zones serve as dynamic interfaces between terrestrial and aquatic ecosystems, playing critical roles in flood regulation, nutrient cycling, biodiversity preservation, and habitat provisioning (Nallaperuma and Asaeda, 2019). The ecological functions of riparian zones result from continuous interactions amongst vegetation dynamics, sediment transport, channel migration, and river hydrodynamics, a process often referred to as bio-hydromorphological feedback (Gurnell et al., 2012; Naiman et al., 2010). This concept is traditionally expressed through the framework of lateral dimension (Hughes, 1997), emphasizing interactions between the river channel, the floodplain, and adjacent terrestrial habitats. Amongst these interactions, lateral connectivity is especially critical, since it enables the redistribution of sediment, nutrients, seeds, and organic materials across the river corridor, thereby supporting vegetation diversity and enhancing ecosystem resilience (Boothroyd et al., 2021; Hughes, 1997; Modi et al., 2022; Ward et al., 2002).

With the increasing availability of large geospatial datasets, the use of remotely sensed information to monitor riverine biohydromorphodynamics has gained momentum (Singh and Vyas, 2022). The Normalized Difference Vegetation Index (NDVI), derived from satellite remote sensing, has become a widely used metric for quantifying vegetation greenness, density, productivity, and phenology (Marchetti et al., 2016; Zeng et al., 2020). Due to the increasing availability and temporal frequency of satellite data, NDVI has facilitated numerous spatiotemporal analyses of riparian vegetation patterns, allowing researchers to link vegetation phenology to hydrological and climatic drivers (Betz et al., 2023; Henriques et al., 2024; Zuo et al., 2022). Riparian vegetation typically exhibits high sensitivity to hydrological fluctuations such as floods, which can alter



40



vegetation structure through significant disturbances such as washout or burial (Edmaier et al., 2011). Conversely, dense vegetation growth within river channels can influence river hydraulics by increasing channel roughness, thereby impeding flow, elevating water levels, and potentially exacerbating flood risks (Bradley et al., 2007; Gao et al., 2022). As a result, balancing ecological integrity with flood conveyance capacity represents a persistent challenge for river management (Stella et al., 2013).

Despite substantial advances in remote sensing technologies, quantitative evaluations of the interplay between flood magnitude,

channel lateral dimension and connectivity, vegetation phenology, and NDVI dynamics remain insufficiently explored,
particularly in steep, gravel-bed rivers subject to frequent flood disturbances. Previous studies have often focused on lowland
rivers or wetlands (Hess et al., 2003; Townsend and Walsh, 2001), leaving gaps in our understanding of steep river systems
where rapid morphological changes and vegetation disturbances frequently occur (Herrmann et al., 2024; Marchetti et al.,
2020). Discussions regarding the application of easily obtained remote sensing data to practical management strategies in river
channels characterized by vegetation overgrowth remain limited. Addressing these gaps is crucial, especially in rivers
characterized by woody vegetation encroachment, significant channel morphology changes, and high flood risks.

This study addresses the following three primary research questions using data from the Chikuma River in Japan, a gravel-bed river characterized by its steep slope and significant riparian vegetation overgrowth:

- (1) How do NDVI dynamics relate to flood magnitude and lateral channel morphology?
- 55 (2) What are the distinct phenological characteristics of riparian vegetation as revealed through NDVI analyses?
 - (3) How can NDVI-derived metrics support practical river management strategies?

By addressing these questions, we explore the potential of NDVI as a reliable indicator of bio-hydromorphological interactions and assess its applicability for flood mitigation and vegetation control planning. The structure of the paper is, as follows. We first introduce datasets and analytical methods, including remote sensing, hydrological records, and topographic data processing. We then evaluate spatial and temporal NDVI patterns in relation to flood magnitude and relative elevation, and we examine the seasonal vegetation phenology. Finally, we discuss the optimal time ("when") and the spatial prioritization ("where") of riparian vegetation management actions.

2 Study Area and Data source

2.1 Study site

The study area for our research was the Chikuma River, located in Nagano Prefecture, Central Japan (**Fig. 1**). Our study focused on a 20-kilometer river reach, extending from 109 km to 89 km upstream of the river mouth. Within this reach, the river has a slope of approximately 1/200 and a representative grain size (d60) of 53 mm, classifying it as a steep, gravel-bed river. Woody vegetation, primarily composed of *Robinia pseudoacacia* and *Salix* species, has extensively encroached in this section of the river, significantly impacting flood management. As a result, periodic, nature-oriented river maintenance practices, including vegetation cutting and river channel excavation, have been implemented for balancing flood conveyance capacity with biodiversity conservation objectives.





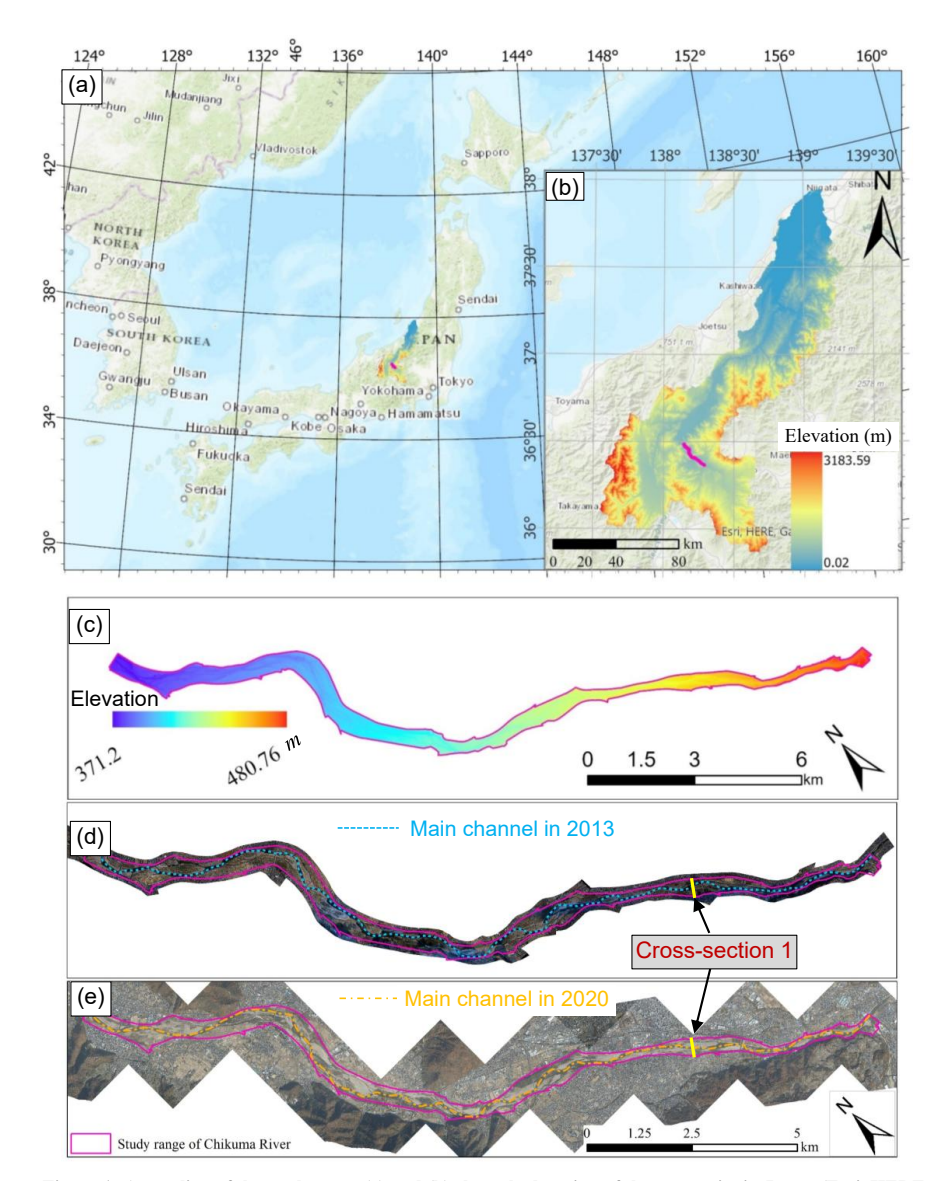


Figure 1: An outline of the study area. (a) and (b) show the location of the target site in Japan (Esri, HERE, Garmin, FAO, NOAA, USGS) and the watershed (Digital Elevation Model (DEM) from the Geospatial Information (GSI) Authority of Japan), respectively; (c) shows the morphology (DEM from the GSI) of the target site; and (d) and (e) provide orthophotos from 2013 and 2020 (Copyright © MLIT in Japan), respectively.

2.2 Data source

80

By considering the application of readily available high-frequency satellite images on grasping riparian vegetation dynamics, a time series of sentinel-2 from 2015 to 2024 was collected. Topographic and hydrological data were additionally obtained to evaluate the dynamics of hydrology and channel lateral morphology.

2.2.1 Sentinel-2 images and NDVI data

For the study, we collected Sentinel-2 satellite imagery (Red, Green, Blue, and Near-Infrared (NIR) bands) at a spatial resolution of 10 m. Given that the minimum and average channel widths at the study reach are approximately 190 and 380 m,



90

95

100

105



respectively, a spatial resolution of 10 m was sufficient to effectively distinguish between vegetation zones, bare gravel bars, and water surfaces. In total, 200, cloud-free, Sentinel-2 images were downloaded from https://browser.dataspace.copernicus.eu/ and processed to compute the NDVI.

2.2.2 Hydrological data

Hydrological records, specifically hourly water level (Fig. 2) measurements during the study period, were obtained from the Water Information System maintained by MLIT, Japan. Data was acquired from the Kuiseke gauging station, located near the center of the study reach. These water level records allowed for the identification of flood timing and magnitude throughout the study period, thus providing critical inputs for investigating the relationship between flow disturbances and vegetation dynamics. Two high-magnitude flood events, referred to as the first and second flood, were identified during the 10-year study period.

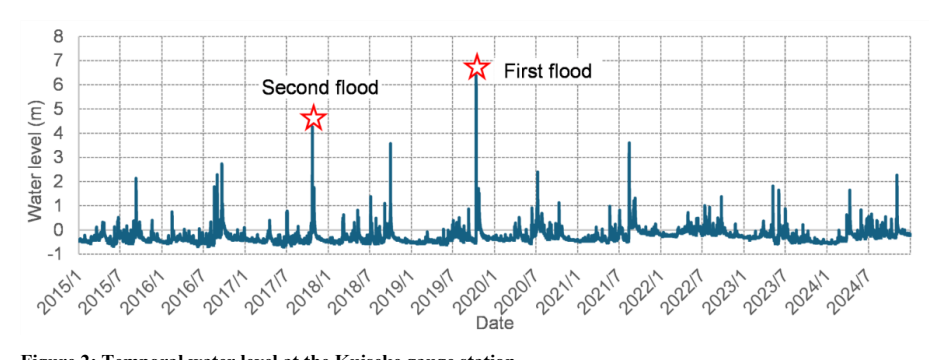


Figure 2: Temporal water level at the Kuiseke gauge station.

2.2.3 Topography data and vegetation height

Topographic information for areas above the water's surface was obtained from a laser profile (LP) survey, which provided the digital elevation model (DEM) and the digital surface model (DSM), with a resolution of 0.5 m. Since the LP sensor does not penetrate water, bathymetric data for submerged areas were derived from cross-sectional surveys conducted at 500 m intervals. LP surveys were conducted in October 2013, December 2019, and November 2020, while cross-sectional surveys were performed in 2013, 2017 and 2019. These datasets revealed dynamic changes in lateral channel morphology (**Fig. 3**) and shifts in the main channel from 2013 to 2019 (**Fig. 1** (d) and (e)). Airborne Lidar Bathymetry (ALB) data surveyed during early December 2024, were also acquired, covering both submerged and non-submerged topographic regions. All of the topographic datasets utilized in this study were provided by the Chikuma River Office of the Ministry of Land, Infrastructure, Transport and Tourism (MLIT), Japan, and are considered reliable and accurate for the purposes of this research.

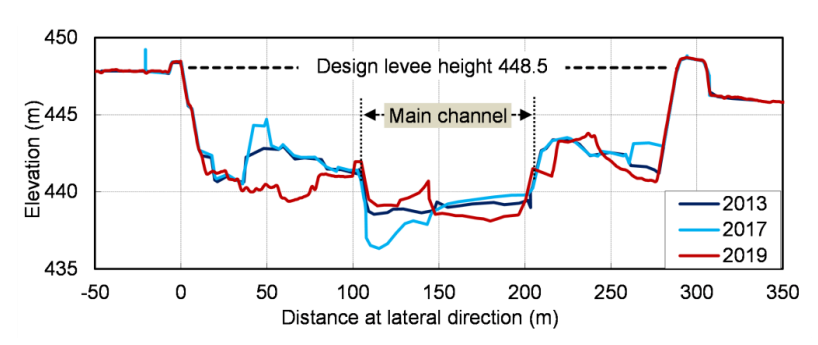


Figure 3: A cross-sectional profile of morphology at Cross-section 1.



120

140

145



110 2.3 The methodology for data analysis

2.3.1 The greenness ratio calculation based on NDVI data

NDVI values for each Sentinel-2 image were generated in ArcGIS Pro using Eq. (1). In previous studies, land cover has commonly been classified into three categories using NDVI thresholds: water (NDVI < 0), bare bars or sparse vegetation (NDVI = 0.0–0.2), and active vegetation (NDVI > 0.2) (Tucker, 1979; Drori et al., 2020). However, in riparian zones, NDVI values can drop below 0.2 during late autumn and winter due to seasonal senescence. As a result, we categorized areas with a NDVI ≤ 0 as water, a NDVI between 0 and 0.2 as bare bars or dormant (non-photosynthesizing) vegetation, and a NDVI > 0.2 as active photosynthesizing vegetation, which we refer to as "greenness" (Tucker, 1979). We specifically focused on NDVI > 0.2, vegetation greenness, for analyzing the interaction between vegetation dynamics, flood magnitude, and phenological characteristics, due to the following points. First, major floods at our study site typically occur during September or October, by which time vegetation has generally recovered from seasonal dormancy and is actively photosynthesizing (NDVI > 0.2). Second, phenological activity, inherently reflecting the growth and expansion of active vegetation, corresponding to NDVI values above 0.2. The greenness ratio is defined as the proportion of area with NDVI > 0.2 relative to total area (Eq. (2)). To quantify the temporal change of NDVI and the greenness ratio during the study period along the channel transect, we introduced the parameter *NDVI*_{vary} and *Green*_{vary}, calculated using Eq. (3):

$$125 NDVI = \frac{NIR - Red}{NIR + Red} (1)$$

$$Greenness\ ratio = \frac{N_{0.2}}{N_{total}} \tag{2}$$

$$\begin{cases} NDVI_{vary} = \sum_{y=2}^{N} \frac{Abs(\overline{NDVI_y} - \overline{NDVI_{y-1}})/\overline{NDVI_{y-1}}}{y-1} \\ Green_{vary} = \sum_{y=2}^{N} \frac{Abs(\overline{Green_y} - \overline{Green_{y-1}})/\overline{Green_{y-1}}}{y-1} \end{cases}$$
(3)

where, $N_{0.2}$ and N_{total} refer to the number of pixels within sentinel-2 imagery where NDVI > 0.2 and the total number of pixels within the target area, respectively.

 $\overline{NDVI_y}$ and $\overline{NDVI_{y-1}}$ represent the average annual maximum NDVI values at each 0.5m relative elevation zone (detailed as described in detail in section 2.3.2) corresponding to y and y-1 years, respectively. $\overline{Green_y}$ and $\overline{Green_{y-1}}$ represent the average annual maximum greenness ratio at each 0.5m relative elevation zone corresponding to y and y-1 years, respectively. N is the total year during the study period. The term "Abs" represents the absolute value of the NDVI difference between two years.

135 **2.3.2** The calculation relative elevation

In this study, we focused on riparian vegetation located between levee banks within the river channel (**Fig. 4**). The conceptual framework of the lateral dimension, which emphasizes interactions between the river channel and riparian vegetation, has been proposed in previous studies (Hughes et al., 1997). While absolute elevation is commonly used to analyze vegetation dynamics at the watershed scale (**Fig. 1**(b)), it typically shows a natural decrease upstream to downstream (**Fig. 1**(c)). However, this longitudinal variation does not adequately capture the spatial patterns of riparian vegetation within the channel when viewed from a lateral dimension perspective.

In this context, since the previous research (Zhu et al., 2023) suggests that relative elevation, defined as the height of floodplain landforms above the water's edge, has a stronger influence on the vegetation distribution within levee banks, relative elevation is proposed as a useful index for characterizing lateral continuity and for examining the relationship between NDVI patterns and topographic characteristics within the river corridor. We specifically define relative elevation as the height above the 95th water level, indicating that the water's surface is at or above this level approximately 95 days per year. Areas below this





elevation are more frequently inundated by river flow, while areas above experience alternating wet and dry conditions that are more conductive for vegetation establishment and persistence. At our study site, riparian vegetation is predominantly distributed above the edge of the 95th flow inundation zone.

150

155

160

165

170



Figure 4: A riparian vegetation cross-sectional distribution (2024 ALB survey results, Copyright © MLIT in Japan).

Riparian vegetation is often considered to be reset following major morphological changes induced by large flood events (Death et al., 2015). Two such significant floods occurred in 2017 and 2019 within the Chikuma River, prompting us to divide the study period into three intervals to better represent the evolving physical environment: Period 1 (2015–2017), Period 2 (2018–2019), and Period 3 (2020–2024).

To calculate relative elevations for each period, we used a combination of topographic datasets. We specifically employed 2013 laser profiling (LP) and cross-sectional survey data for Period 1, 2013 LP and 2017 cross-sectional data for Period 2, and 2024 airborne lidar bathymetry (ALB) data for Period 3. Since floodplain morphology was assumed to largely remain unchanged, with most morphological adjustments occurring within the main channel (**Fig. 3**), the 2013 LP dataset was reused for both Periods 1 and 2.

The 95th water level, which varies in response to morphological dynamics, was calculated for each analysis period using the two-dimensional hydraulic simulation model Nays2DH (Shimizu et al., 2020). Relative elevation was then derived by subtracting the simulated water level from topographic elevation (**Fig. 5**). For detailed analyses, resulting relative elevation values were classified into two schemes: one with 50 classes at 0.1 m intervals, and another with 10 classes at 0.5 m intervals, covering the range from 0 to 5 m.

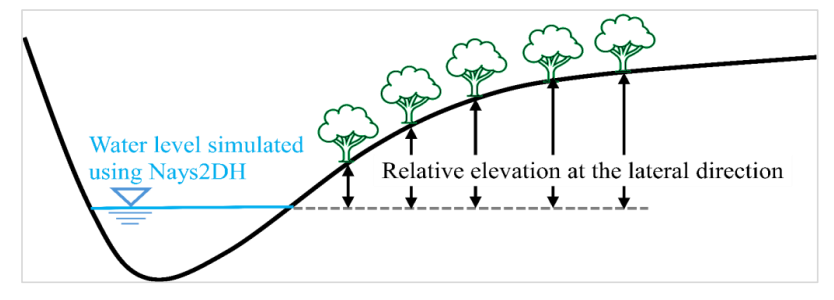


Figure 5: Conceptual diagram of relative elevation in the lateral direction.

2.3.3 Characterizing riparian vegetation NDVI phenomena

Phenological characteristics of riparian vegetation across dryland regions have been analyzed using Google Earth Engine; for example, McMahon et al. (2024) mapped riparian woodlands and land-surface phenology from Sentinel-2 time series in a cloud-based workflow. A discussion of the phenological characteristics of riparian vegetation specifically within frequently disturbed river channels is relatively limited. In this study, we sought to clarify the phenological patterns of riparian vegetation



175

180

185

190

195

200

205

210



by utilizing time-series NDVI data extracted from Sentinel-2 satellite imagery. To reduce the confounding effects of flow and morphological changes induced by major floods, and to highlight inherent ecological patterns of vegetation, we calculated monthly averaged NDVI values for each year over a 10-year period. These annual monthly-average values were then analyzed to identify and interpret ecological characteristics of in-channel riparian vegetation. To better understand the environmental drivers influencing these phenological patterns (Wang et al., 2024), we, additionally, collected and integrated temperature and precipitation data from the Ueda meteorological station (https://www.data.jma.go.jp/stats/etrn/index.php?prec_no=48&block_no=0402&year=&month=&day=&view=) into our analysis. Yearly averages of monthly mean temperature, monthly maximum temperature, and monthly accumulated precipitation were calculated for the period from 2015 to 2024.

3 Results and Discussion

3.1 NDVI and hydromorphodynamics

3.1.1 Spatial-temporal NDVI and the hydrodynamics of water level

Figure 6 presents 10 hour accumulated water level alongside the greenness ratio at different relative elevations. The figure demonstrates the influence of the catastrophic flood on vegetation. Fluctuations in vegetation greenness were closely associated with both flood magnitude and relative elevation. The greenness ratio consistently declined following the occurrence of notable annual maximum floods, particularly those in 2017, 2018, 2019, and 2021. The severity of these floods, based on return periods, was as follows: 2019 (~50-year), 2017 (~10-year), 2021 (~5-year), and 2018 (~3-year). The observed reduction in greenness occurred across different lateral relative elevation ranges: 0–5 m (2019), 0–3 m (2017), 0–3 m (2021), and 0–2 m (2018). Although the lateral extent of greenness reduction during the 2021 and 2017 floods was similar, the magnitude of the reduction was greater in 2017. Overall, the magnitude of greenness declines mirrored flood severity: the most substantial reduction occurred during the 2019 flood, followed by the 2017 event, with smaller but still observable declines in 2021 and 2018, respectively.

The results clearly indicate that greenness at lower relative elevations fluctuates more strongly than at higher elevations. For example, significant declines in greenness were observed within the 0–3 m relative elevation range following the 2017 and 2021 annual maximum floods, while vegetation above 3 m largely remained unaffected by floods of similar magnitude, indicating that flood magnitude alone does not fully explain the dynamics of riparian vegetation disturbance. Instead, lateral channel morphology, particularly relative elevation, plays a critical role in shaping vegetation resistance and recovery (Death et al., 2015; Herrmann et al., 2024). **Figure 6** illustrates a clear distinction in riparian vegetation responses that jointly depend on flood magnitude (closely linked to specific return periods) and relative elevation, highlighting the importance of integrating hydrological and morphological factors when assessing vegetation vulnerability and planning management strategies.

Figure 7 presents annual maximum NDVI values alongside corresponding water level records. Notably, declines in maximum NDVI were observed in 2018 and 2020, likely reflecting the impact of substantial flood-induced vegetation removal in the preceding years (2017 and 2019, respectively). High-magnitude floods (with return periods of five years or more) tend to cause widespread vegetation removal (Nallaperuma and Asaeda, 2020) and can drastically reshape channel morphology, effectively reset riparian vegetation structure, and temporarily improve channel conveyance capacity (Death et al., 2015; Stella et al., 2013). In contrast, although vegetation reduction at relative elevations of 0–2 m was observed during the 2018 and 2021 flood events, NDVI increased again in 2019 and 2022. This pattern suggests rapid post-flood regrowth, particularly following moderate floods. Such events typically result in limited vegetation removal but may stimulate regrowth through enhanced nutrient availability and reduced interspecies competition (Greet et al., 2011; Herrmann et al., 2024).





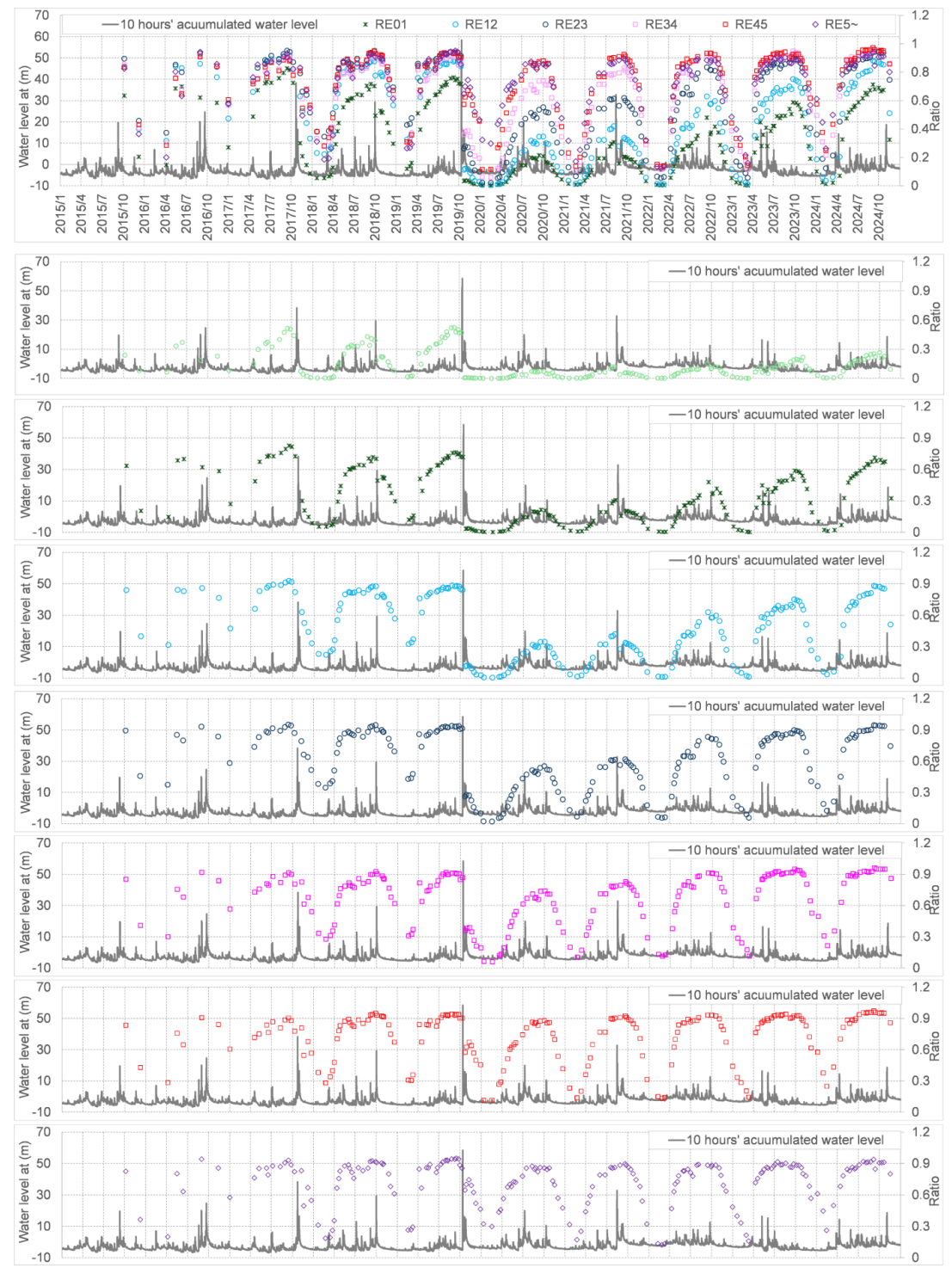


Figure 6: Spatiotemporal vegetation greenness and hydro-morphology dynamics.



220

230

235



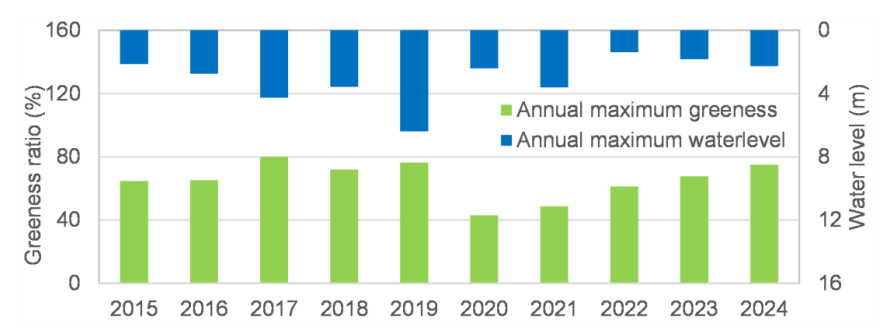


Figure 7: Relationship between annual maximum greenness and water level.

3.1.2 The annual maximum greenness ratio and the NDVI distribution along the transect

We further examined the temporal dynamics of riparian vegetation greenness over a 9-year period from 2016 to 2024, excluding 2015 due to limited NDVI data availability. The analysis focused on annual maximum NDVI across varying relative elevations. The maximum greenness ratio was extracted and analyzed because NDVI typically peaks between July and October at the study site, the primary growing season for both herbaceous and woody vegetation (Pettorelli et al., 2005). During this period, vegetation cover is most fully developed and NDVI values above 0.2 reliably correspond to active green vegetation, making NDVI > 0.2 (Drori et al., 2020) a suitable threshold for estimating vegetation cover. The maximum greenness ratio was taken as a proxy for the annual peak in vegetation cover.

Figure 8 illustrates the lateral distribution of the greenness ratio, measured from the shoreline (relative elevation = 0 m) to the levee bank (above 5 m). A clear increasing trend in the greenness ratio was observed from the river's edge up to approximately 5 m in relative elevation. Beyond this elevation, however, the greenness ratio declined, likely due to the presence of artificial structures near the levee banks, which limit suitable conditions for vegetation establishment.

The relationship between greenness ratio and relative elevation was modelled using an empirical function (Eq. (4)), with the fitted curves for each year shown in **Fig. 8**. The parameters L, h_0 and k utilized in the model are summarized in **Table 1**. Among the parameters, h_0 , which indicates the relative elevation of the greenness ratio to be reached at 50%, was found to vary with flood conditions from the preceding year. **Figure 9** shows the temporal variation of h_0 and the annual maximum water level from 2016 to 2024. A sharp decline in h_0 was observed during 2020, indicating that riparian vegetation was likely removed at a lower relative elevation, correspondingly with the effect of the mega flood in 2019. Since 2021, h_0 has gradually increased, suggesting a recovery process in riparian vegetation from lower relative elevation toward the higher floodplain.

$$Green(h) = \frac{L}{1 + exp\left(-k(h - h_0)\right)} \tag{4}$$

G(h): Greenness ratio with a relationship to relative elevation (h)

L: Maximum greenness ratio, h_0 : the relative elevation at which the greenness ratio equals 0.5 (50%),

k: Steepness parameter



250

255

260



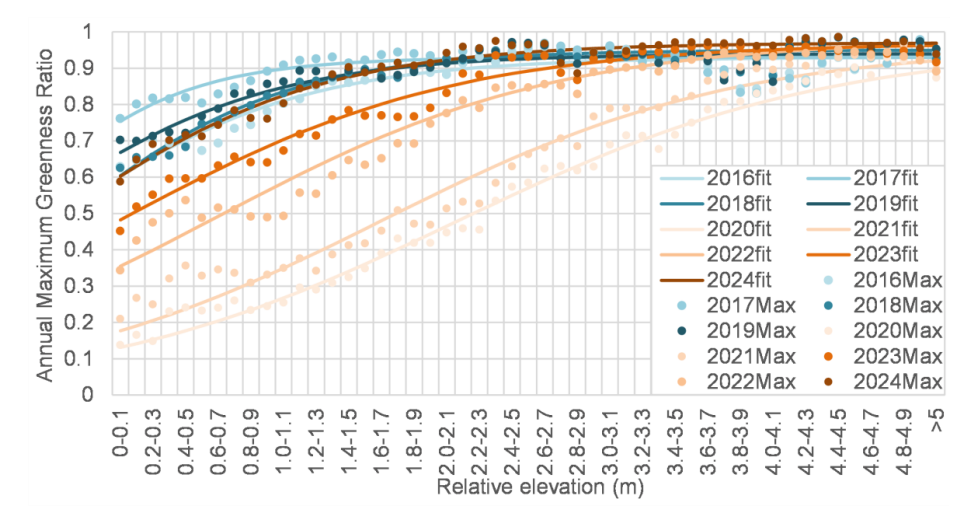


Figure 8: Annual maximum greenness ratio along the transect.

Table 1: Parameters utilized in the fitting curve.

| Parameter | 2016 | 2017 | 2018 | 2019 | 2020 | 2021 | 2022 | 2023 | 2024 |
|-----------|-------|-------|-------|-------|------|------|------|------|-------|
| L | 0.93 | 0.93 | 0.95 | 0.94 | 0.96 | 0.96 | 0.98 | 0.97 | 0.97 |
| h_0 | -0.42 | -0.72 | -0.34 | -0.63 | 2.12 | 1.65 | 0.64 | 0.06 | -0.35 |
| k | 1.3 | 1.89 | 1.43 | 1.32 | 0.89 | 0.93 | 0.96 | 0.98 | 1.24 |

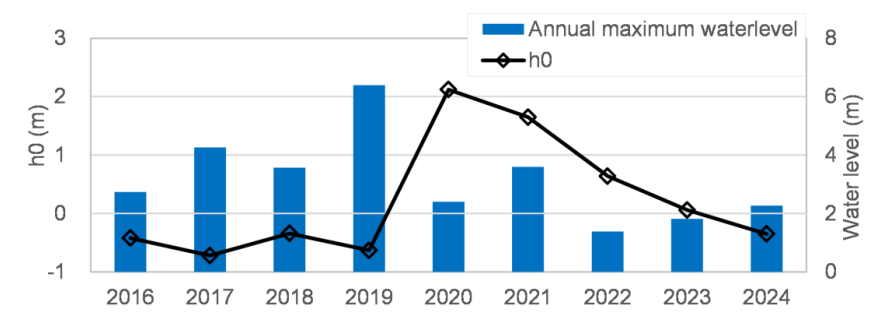


Figure 9: Relationship between h_0 and annual maximum water level.

The greenness ratio reflects the presence or absence of vegetation based on an NDVI threshold (> 0.2), serving as a binary indicator of vegetated area. In contrast, NDVI values themselves provide more detailed information on vegetation health and type, with higher values typically indicating denser and healthier vegetation. At peak summer greenness, trees generally show higher NDVI than grasses due to greater leaf area and NIR reflectance; accordingly, NDVI helps discriminate woody versus herbaceous vegetation here. As such, following the greenness ratio analysis, NDVI values were further analyzed to gain insight into vegetation condition and type composition. **Figure 10** shows annual maximum NDVI along the transect at different relative elevations. Distinct differences in NDVI distribution patterns along transects were observed between the periods 2016–2019 and 2020–2024. During 2016–2019, NDVI values increased with relative elevation from 0 m up to approximately 3 m, and then decreased between 3 and 5 m. Prominent NDVI peaks were identified around 1.5 and 3.5 m. In contrast, during 2020–2024, NDVI exhibited a more gradual and consistent increase from 0 to 5 m, indicating a different spatial pattern of vegetation greenness. Two main factors may explain the observed NDVI distribution patterns: (1) the lateral distribution of vegetation species, and (2) the preferred physical environment for vegetation growth.

In this study, the ratio of each vegetation type along the transect was calculated based on Environment Information Map 2018 and relative elevation. Environment Information Map 2018 records the vegetation species distribution, and was surveyed by



270

275

280

285



the Ministry of Land, Infrastructure, Transport and Tourism (MLIT). As shown in **Fig. 11**, grass-dominated zones (green line) and tree-dominated zones (red line) spatially differed during 2018. Similar peaked lateral distributions of vegetation types have frequently been reported in previous studies (Camporeale and Ridolfi, 2006; Carter Johnson et al., 1995). At the current study site, Robinia pseudoacacia, the dominant riparian tree species, is primarily distributed between 2.0 and 4.0 m in relative elevation. Since riparian trees typically exhibit higher NDVI values than grasses, the concentration of Robinia in this elevation range likely contributed to the distinct NDVI peaks observed from 2016–2019.

The physical environment across the elevation gradient additionally plays a critical role. Vegetation at lower elevations (<1.5 m) is more frequently disturbed or washed away, even during moderate flood events, limiting establishment and biomass accumulation. In contrast, vegetation at higher elevations (>3.5 m) may experience insufficient inundation, which can reduce soil moisture and nutrient inputs, ultimately constraining growth (Marchetti et al., 2020; Modi et al., 2022). Therefore, the intermediate elevation band between 1.5 and 3.5 m offers a relatively balanced environment with suitable disturbance frequency and resource availability, supporting healthier vegetation growth and contributing to higher NDVI within this zone. Following the 2019 flood, much of the riparian vegetation below 4 m, including *Robinia pseudoacacia*, was removed. From 2020 to 2024, *Robinia* had not yet re-established as the dominant species within this elevation range. As a result, the NDVI profile during this period lacked the distinct peaks previously observed between 1.5 and 3.5 m, instead exhibiting a smoother upward trend across the transect. In particular, NDVI values in 2020 within the 2.0–3.0 m elevation band were significantly lower than those above 3.5 m, suggesting that the lower zones were still in an early recovery stage. However, from 2020 to 2024, the difference in NDVI between these two elevation zones gradually diminished. This trend likely reflects a transitional phase characterized by the progressive establishment of early successional riparian tree species, which are beginning to recolonize lower elevation areas following large-scale disturbance.



Figure 10: Averaged annual maximum NDVI for each 0.5 m RE zone along the transect.

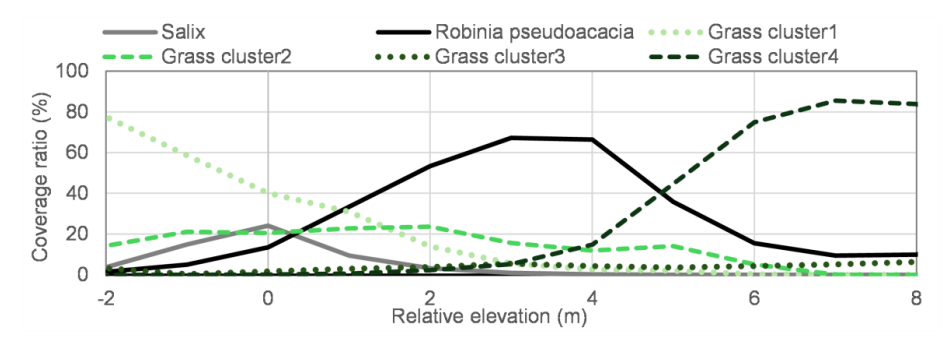


Figure 11: Vegetation type and its coverage ratio along the transect.



295

300

305



3.2 Seasonal dynamics of riparian greenness

We calculated the monthly averaged greenness ratio (**Fig. 12**) from NDVI data extracted from approximately 200 Sentinel-2 images. Since only two images were available for 2015, that year was excluded from the analysis. From March to June, the greenness ratio steadily increased with rising temperatures, and precipitation created favorable conditions for photosynthesis. However, the upward trend slowed during July and August, a trend that may have been caused by elevated temperatures and high cumulative precipitation that stimulated respiratory activity more than photosynthesis (**Fig. 13**). As temperatures and rainfall moderated from mid-summer peaks, riparian vegetation entered a secondary growth phase, and the greenness index reached a maximum during September. A post-October decline in the greenness index correlated to reduced temperatures and precipitation regimes, leading to diminished photosynthetic activity. Overall, we propose a cosine curve model (Eq. (5)), with ecologically interpretable parameters: *A* (overall average level), *B* (amplitude), and Ø (timing of maximum occurs), to express the seasonal cycling process of monthly greenness. "A" and "B" indicate the year-round baseline of greenness and the intensity of the seasonal swing in greenness, respectively. A smaller "B" indicates evergreen dominance or disturbance-limited phenology, whereas a larger "B" indicates strong leaf-out. The peak month ("Ø") shifted one month earlier than expected, occurring in August instead of September.

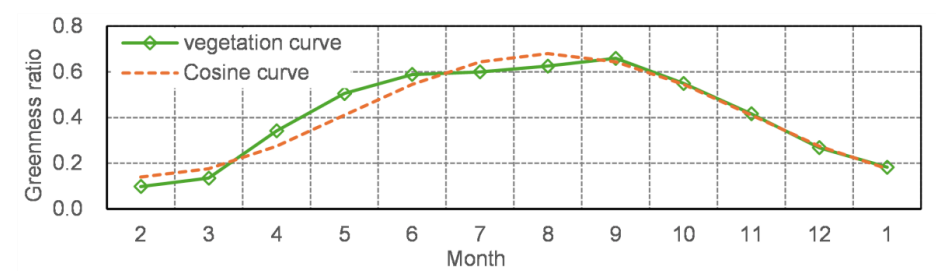


Figure 12: Seasonal dynamics of greenness ratio.

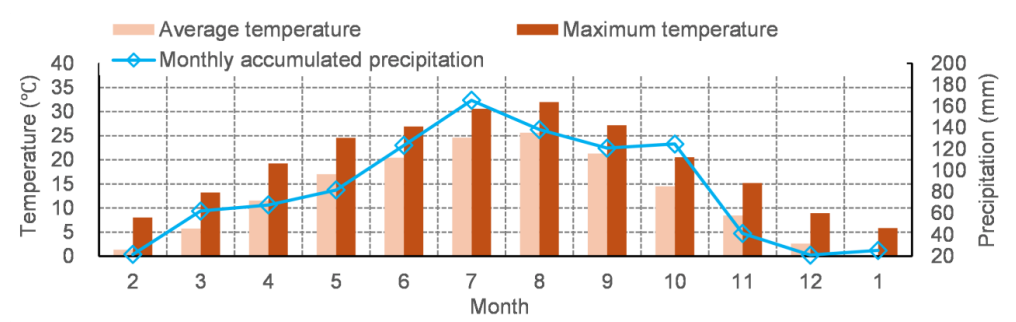


Figure 13: The seasonal dynamics of temperature and precipitation.

$$V(m) = A + B\cos(\omega(m - \emptyset)) = 0.41 + 0.27\cos(\frac{\pi}{6} \times (m - 8))$$
(5)

310 A: the overall average level (offset) (A = 0.41)

B: Amplitude (B = 0.27)

m: Month

 ω : corresponding to the annual cycle ($\omega = \frac{2\pi}{12} = \frac{\pi}{6}$)

Ø: the phase that determines the month in which the maximum occurs



330

335

340

345

350



315 Riparian vegetation within river channels is subject to more complex environmental conditions than vegetation in mountainous or urban landscapes. In addition to climate factors, hydro-morphodynamic variables, including relative elevation and flood magnitude, strongly influence in-channel vegetation dynamics (Betz et al., 2023). Despite these complexities, a harmonic modeling approach (Bradley et al., 2007) remained effective for analyzing seasonal NDVI trends over medium- to long-term timescales. Higher NDVI values, reflecting denser vegetation, are associated with increased channel roughness, which can 320 reduce flow capacity and raise water levels (AI Mehedi et al., 2024). This, in turn, elevates the risk of floodplain inundation. At the Chikuma River study site, NDVI values typically peak in August or September, coinciding with the end of the growing season. However, major flood events in this region, often triggered by typhoons, tend to occur in late September or October. This seasonal overlap implies that peak vegetation development may align with the onset of extreme flood events, thereby posing elevated risks to embankment safety and increasing the urgency for targeted vegetation management interventions. 325 Given its 10 m spatial resolution and the inherent upper limit of NDVI ≤ 1 (Redowan and Kanan, 2012), accurately estimating vegetation height and density remains challenging when using Sentinel-2 data. Therefore, additional high-resolution surveys, such as ALB, are essential for capturing finer vegetation details. Ideally, these surveys should be conducted in August or September, when vegetation is at or near its peak and can support hydraulic modelling with robust vegetation data. However,

3.3 Riverine management implications

both hydraulic parameter accuracy and geomorphological assessment needs.

Effective riparian vegetation management requires addressing two key dimensions: identifying the optimal time ("when") and the spatial prioritization ("where") of management actions. Optimal timing involves understanding when vegetation expands, while spatial prioritization refers to identifying locations within river channels where management activities (such as vegetation cutting or thinning) would yield the most significant benefits in terms of flood conveyance and ecosystem stability.

to map morphological features, ALB is often conducted in November or December, thus requiring careful scheduling to align

3.3.1 The timing of vegetation management

The long-term dynamics of NDVI and its response to hydrological disturbances offer valuable insights for determining the optimal timing of vegetation management in river channels. High-magnitude floods (with return periods of five years or more) often lead to widespread vegetation removal, effectively resetting riparian vegetation structure and temporarily enhancing flow capacity (Death et al., 2015; Stella et al., 2013). In contrast, smaller floods (return periods of less than three years) typically cause limited vegetation disturbance. In such cases, vegetation tends to expand in the following year, potentially resulting in overgrowth that elevates water levels and increases the risk of embankment overtopping. Therefore, proactive vegetation management, such as selective cutting or thinning, is necessary for maintaining adequate flow conveyance capacity.

Our long-term NDVI analysis also revealed distinct patterns for post-disturbance vegetation recovery. Although NDVI values sharply declined after the 2019 mega flood, a steady regrowth trend was observed between 2020 and 2024, with the maximum greenness ratio nearly returning to pre-flood levels by 2024. These findings underscore the importance of integrating both short-term flood impacts and long-term successional dynamics into riparian vegetation management strategies (Herrmann et al., 2024; Stella et al., 2013). Moreover, the spatial and temporal patterns of NDVI recovery provide useful indicators of vegetation recruitment characteristics and growth rates, which could provide information regarding the development of process-based riparian vegetation models (Nallaperuma and Asaeda, 2020; Toda et al., 2020).

3.3.2 Spatial prioritization for management actions

Figure 14 illustrates the 9-year period variations of NDVI and the greenness ratio along the transect of the river channel. Lower-elevation zones (<1.5 m) exhibited rapid vegetation recovery post-disturbance, yet frequently experienced washouts from moderate floods, necessitating regular management interventions to maintain adequate flow capacity (Death et al., 2015;



360

365

370

375

380



Nallaperuma and Asaeda, 2020). Conversely, higher-elevation zones (> 3.5 m) harbor stable vegetation that typically resists disturbances from common flood events but significantly influences flow conveyance during infrequent, high-magnitude floods, thereby requiring periodic but strategically timed interventions (Herrmann et al., 2024; Stella et al., 2013). Intermediate-elevation zones (1.5 – 3.5 m) presented moderate vegetation dynamics, experiencing moderate fluctuations in vegetation density and growth rates. Vegetation within these zones impacts flow capacity for both medium and large flood events, aligning with findings from previous research indicating the critical importance of managing vegetation at moderate elevations for comprehensive flood mitigation (Marchetti et al., 2020; Modi et al., 2022). Thus, targeted management within these intermediate zones provides balanced flood-risk reduction, effectively maintaining ecosystem stability while addressing both regular and extreme flood conveyance needs.

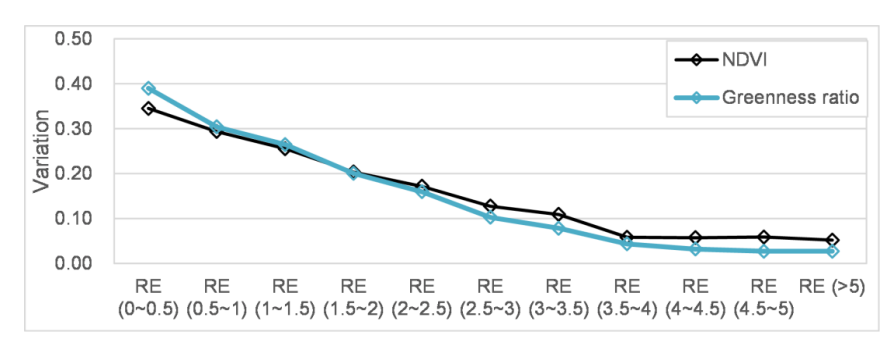


Figure 14: Averaged variation of NDVI and greenness ratio from 2016 to 2024.

4 Conclusions

In this study, we quantified how riparian vegetation NDVI varies with flood magnitude, relative elevation, and season along a steep, gravel-bed reach using 200 Sentinel-2 satellite images (2015–2024). Vegetation at lower elevations (0–3 m above the 95th-percentile stage) was most disturbance-prone, whereas higher zones were comparatively stable. Cross-channel transects showed a logistic relation between greenness (NDVI > 0.2) and relative elevation; the 50% greenness elevation shifted after large floods and gradually recovered, indicating reorganized vegetation bands during post-flood succession. Monthly NDVI revealed a clear phenology with late-summer peaks (Aug–Sep), overlapping the regional flood season (Sep–Oct) when vegetation-induced roughness can most influence conveyance. Taken together, spatiotemporal NDVI provides an efficient indicator of bio-hydromorphodynamic behavior and yields actionable guidance for management: where to prioritize control, at intermediate elevations (1.5–3.5 m) that most influence conveyance yet remain manageable; and when to act, near peak greenness or immediately after disturbance, consistent with flood-risk timing.

Author contribution

YZ planned the study and methodology; YZ and RZ performed the investigation; YZ conducted the formal analysis and curated the data (with additional data curation by YT); YZ wrote the manuscript draft; YT and RZ reviewed and edited the manuscript; YT provided validation and acquired funding.

Competing interests

The authors declare that they have no known competing financial interests or personal relationships that could have appeared to influence the work reported in this paper.





385 Data availability

Sentinel-2 imagery used in this study is available at https://doi.org/10.5281/zenodo.17240522 (ZHOU, 2025). The temporal water level was download from the https://www.data.jma.go.jp/stats/etrn/. The vegetation type data was downloaded from the https://www.nilim.go.jp/lab/fbg/ksnkankyo/. Topography data of ALB and LP will be made available on request.

390 Acknowledgements

We gratefully acknowledge the provision of the LP, ALB data by the Chikuma River office.

Financial support

The study was partially funded by JSPS KAKENHI, grants 24K17354 and 25K01333.

References

- Al Mehedi, M. A., Saki, S., Patel, K., Shen, C., Cohen, S., Smith, V., ... & Lawson, K.: Spatiotemporal variability of channel roughness and its substantial impacts on flood modeling errors, Earth's Future, 12(7), e2023EF004257, doi: 10.1029/2023EF004257, 2024.
 - Bendix, J., Stella, J.C.: Riparian vegetation and the fluvial environment: a biogeographic perspective, Treatise on Geomorphology, 53–74. doi: 10.1016/B978-0-12-374739-6.00322-5, 2013.
- Betz, F., Lauermann, M., and Egger, G.: Biogeomorphology from space: Analyzing the dynamic interactions between hydromorphology and vegetation along the Naryn River in Kyrgyzstan based on dense satellite time series, Remote Sens. Environ., 299, 113890, doi:10.1016/j.rse.2023.113890, 2023.
 - Boothroyd, R. J., Nones, M., and Guerrero, M.: Deriving planform morphology and vegetation coverage from remote sensing to support river management applications, Front. Environ. Sci., 9, 657354, doi:10.3389/fenvs.2021.657354, 2021.
- Bradley, B. A., Jacob, R. W., Hermance, J. F., and Mustard, J. F.: A curve fitting procedure to derive inter-annual phenologies from time series of noisy satellite NDVI data, Remote Sens. Environ., 106, 137–145, doi:10.1016/j.rse.2006.08.002, 2007.
 Camporeale, C. and Ridolfi, L.: Riparian vegetation distribution induced by river flow variability: A stochastic approach,
 - Camporeate, C. and Ridoffi, L.: Riparian Vegetation distribution induced by river flow variability: A stochastic approach, Water Resour. Res., 42, W10433, doi:10.1029/2006WR004933, 2006.
 - Carter Johnson, W.C., Dixon, M.D., Simons, R., Jenson, S., Larson, K.: Mapping the response of riparian vegetation to possible flow reductions in the Snake River, Idaho, Geomorphology. 13, 159–173. doi:10.1016/0169-555X(95)00048-A, 1995.
 - Death, R. G., Fuller, I. C., and Macklin, M. G.: Resetting the river template: The potential for climate-related extreme floods to transform river geomorphology and ecology, Freshw. Biol., 60, 2477–2496, doi:10.1111/fwb.12639, 2015.
 - Drori, R., Dan, H., Sprintsin, M., & Sheffer, E.: Precipitation-sensitive dynamic threshold: A new and simple method to detect and monitor forest and woody vegetation cover in sub-humid to arid areas, Remote Sensing, 12(8), 1231.
- 415 doi:10.3390/rs12081231, 2020.

- Edmaier, K., Burlando, P., & Perona, P.: Mechanisms of vegetation uprooting by flow in alluvial non-cohesive sediment, Hydrology and Earth System Sciences, 15(5), 1615-1627. doi:10.5194/hess-15-1615-2011, 2011.
- Egger, G., Politti, E., Woo, H., Cho, K.-H., Park, M., Cho, H., Benjankar, R., Lee, N.-J., Lee, H.: Dynamic vegetation model as a tool for ecological impact assessments of dam operation, J. Hydro-Environ. Res. 6, 151–161. doi:
- 420 10.1016/j.jher.2012.01.002, 2012.





- Gao, P., Li, Z., You, Y., Zhou, Y., and Piégay, H.: Assessing functional characteristics of a braided river in the Qinghai-Tibet Plateau, China, Geomorphology, 403, 108180, doi:10.1016/j.geomorph.2022.108180, 2022.
- Greet, J., et al.: Floodplain inundation frequency and riparian vegetation dynamics in an unregulated river: implications for vegetation management, Ecohydrology, 4, 234–247, doi:10.1002/eco.148, 2011.
- Gurnell, A. M., Bertoldi, W., and Corenblit, D.: Changing river channels: The roles of hydrological processes, plants and pioneer fluvial landforms in humid temperate, mixed load, gravel bed rivers, Earth-Sci. Rev., 111, 129–141, doi:10.1016/j.earscirev.2011.11.005, 2012.
 - Henriques, M., McVicar, T. R., Holland, K. L., and Daly, E.: Monitoring spatially heterogeneous riparian vegetation around permanent waterholes: A method to integrate LiDAR and Landsat data for enhanced ecological interpretation of Landsat fPAR time-series, Remote Sens. Environ., 315, 114382, doi:10.1016/j.rse.2024.114382, 2024.
- Herrmann, M., Schmidt-Riese, E., Bäte, D. A., Kempfer, F., Fassnacht, F. E., and Egger, G.: Satellite-observed flood indicators are related to riparian vegetation communities, Ecol. Indic., 166, 112313, doi:10.1016/j.ecolind.2024.112313, 2024.

 Hess, L. L., Melack, J. M., Novo, E. M., Barbosa, C. C., and Gastil, M.: Dual-season mapping of wetland inundation and
 - vegetation for the central Amazon basin, Remote Sens. Environ., 87, 404–428, doi:10.1016/j.rse.2003.04.001, 2003.
- Hughes, F. M.: Floodplain biogeomorphology, Prog. Phys. Geogr., 21, 501–529, doi:10.1177/030913339702100402, 1997.
 Johnson, W. C., Dixon, M. D., Simons, R., Jenson, S., and Larson, K.: Mapping the response of riparian vegetation to possible flow reductions in the Snake River, Idaho, Geomorphology, 13, 159–173, doi:10.1016/0169-555X(95)00048-A, 1995.
 Marchetti, Z. Y., Minotti, P. G., Ramonell, C. G., Schivo, F., and Kandus, P.: NDVI patterns as indicator of morphodynamic activity in the middle Paraná River floodplain, Geomorphology, 253, 146–158, doi:10.1016/j.geomorph.2015.10.003, 2016.
- 440 Marchetti, Z. Y., Ramonell, C. G., Brumnich, F., Alberdi, R., and Kandus, P.: Vegetation and hydrogeomorphic features of a large lowland river: NDVI patterns summarizing fluvial dynamics and supporting interpretations of ecological patterns, Earth Surf. Process. Landf., 45, 694–706, doi:10.1002/esp.4766, 2020.
 - McMahon, C. A., Roberts, D. A., Stella, J. C., Trugman, A. T., Singer, M. B., and Caylor, K. K.: A river runs through it: Robust automated mapping of riparian woodlands and land surface phenology across dryland regions, Remote Sens. Environ.,
- 445 305, 114056, doi:10.1016/j.rse.2024.114056, 2024.
 - Modi, A., Kapoor, V., and Tare, V.: River space: A hydro-bio-geomorphic framework for sustainable river-floodplain management, Sci. Total Environ., 812, 151470, doi:10.1016/j.scitotenv.2021.151470, 2022.
 - Naiman, R. J., Decamps, H., and McClain, M. E.: Riparia: ecology, conservation, and management of streamside communities, Elsevier, 2010.
- Nallaperuma, B. and Asaeda, T.: Long-term changes in riparian forest cover under a dam induced flow scheme: the accompanying a numerical modelling perspective, J. Ecohydraul., doi:10.1080/24705357.2019.1663714, 2019.
 - Nallaperuma, B. and Asaeda, T.: The long-term legacy of riparian vegetation in a hydrogeomorphologically remodelled fluvial setting, River Res. Appl., 36, 1690–1700, doi:10.1002/rra.3665, 2020.
 - Pettorelli, N., Vik, J. O., Mysterud, A., Gaillard, J. M., Tucker, C. J., and Stenseth, N. C.: Using the satellite-derived NDVI to
- assess ecological responses to environmental change, Trends Ecol. Evol., 20, 503–510, doi:10.1016/j.tree.2005.05.011, 2005. Redowan, M. and Kanan, A. H.: Potentials and limitations of NDVI and other vegetation indices (VIs) for monitoring vegetation parameters from remotely sensed data, Bangladesh Res. Pub. J., 7, 291–299, 2012.
 - Shimizu, Y., Nelson, J., Arnez Ferrel, K., Asahi, K., et al.: Advances in computational morphodynamics using the International River Interface Cooperative (iRIC) software, Earth Surf. Process. Landf., 45, 11–37, doi:10.1002/esp.4653, 2020.
- Singh, A. and Vyas, V.: A review on remote sensing application in river ecosystem evaluation, Spatial Inf. Res., 30, 759–772, doi:10.1007/s41324-022-00470-5, 2022.





- Stella, J. C., Rodríguez-González, P. M., Dufour, S., and Bendix, J.: Riparian vegetation research in Mediterranean-climate regions: common patterns, ecological processes, and considerations for management, Hydrobiologia, 719, 291–315, doi:10.1007/s10750-012-1304-9, 2013.
- Toda, Y., Zhou, Y., and Sakai, N.: Modeling of riparian vegetation dynamics and its application to the sand-bed river, J. Hydro-Environ. Res., 30, 3–13, doi:10.1016/j.jher.2019.09.003, 2020.
 - Townsend, P. A. and Walsh, S. J.: Remote sensing of forested wetlands: application of multitemporal and multispectral satellite imagery to determine plant community composition and structure in southeastern USA, Plant Ecol., 157, 129–149, doi:10.1023/A:1013999513172, 2001.
- Tucker, C. J.: Red and photographic infrared linear combinations for monitoring vegetation, Remote Sens. Environ., 8, 127–150, doi:10.1016/0034-4257(79)90013-0, 1979.
 - Wang, B., Si, J., Jia, B., He, X., Zhou, D., Zhu, X., and Bai, X.: Monitoring spatial-temporal variability of vegetation coverage and its influencing factors in the Yellow River source region from 2000 to 2020, Remote Sens., 16, 24772, doi:10.3390/rs16244772, 2024.
- 475 Ward, J. V., Tockner, K., Arscott, D. B., and Claret, C.: Riverine landscape diversity, Freshw. Biol., 47, 517–539, doi:10.1046/j.1365-2427.2002.00893.x, 2002.
 - Zeng, L., Wardlow, B. D., Xiang, D., Hu, S., and Li, D.: A review of vegetation phenological metrics extraction using time-series, multispectral satellite data, Remote Sens. Environ., 237, 111511, doi:10.1016/j.rse.2019.111511, 2020.
 - Zhu, R., Tsubaki, R., and Toda, Y.: Effects of vegetation distribution along river transects on the morphology of a gravel bed braided river, Acta Geophys., 71, 1–16, doi:10.1007/s11600-023-01075-8, 2023.
 - Zuo, Y., Li, Y., He, K., and Wen, Y.: Temporal and spatial variation characteristics of vegetation coverage and quantitative analysis of its potential driving forces in the Qilian Mountains, China, 2000–2020, Ecol. Indic., 143, 109429, doi:10.1016/j.ecolind.2022.109429, 2022.